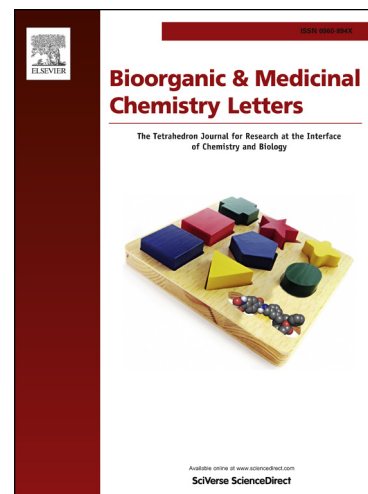


## Accepted Manuscript

Acyl dihydropyrazolo[1,5-*a*]pyrimidinones as metabotropic glutamate receptor 5 positive allosteric modulators

Chrysa Malosh, Mark Turlington, Thomas M. Bridges, Jerri M. Rook, Meredith J. Noetzel, Paige N. Vinson, Thomas Steckler, Hilde Lavreysen, Claire Mackie, José M. Bartolomé-Nebreda, Susana Conde-Ceide, Carlos M. Martínez-Vituro, María Piedrafita, M. Rosa Sánchez-Casado, Gregor J. Macdonald, J. Scott Daniels, Carrie K. Jones, Colleen M. Niswender, P. Jeffrey Conn, Craig W. Lindsley, Shaun R. Stauffer



PII: S0960-894X(15)30118-9  
DOI: <http://dx.doi.org/10.1016/j.bmcl.2015.10.009>  
Reference: BMCL 23165

To appear in: *Bioorganic & Medicinal Chemistry Letters*

Received Date: 7 August 2015  
Revised Date: 30 September 2015  
Accepted Date: 5 October 2015

Please cite this article as: Malosh, C., Turlington, M., Bridges, T.M., Rook, J.M., Noetzel, M.J., Vinson, P.N., Steckler, T., Lavreysen, H., Mackie, C., Bartolomé-Nebreda, J.M., Conde-Ceide, S., Martínez-Vituro, C.M., Piedrafita, M., Rosa Sánchez-Casado, M., Macdonald, G.J., Scott Daniels, J., Jones, C.K., Niswender, C.M., Jeffrey Conn, P., Lindsley, C.W., Stauffer, S.R., Acyl dihydropyrazolo[1,5-*a*]pyrimidinones as metabotropic glutamate receptor 5 positive allosteric modulators, *Bioorganic & Medicinal Chemistry Letters* (2015), doi: <http://dx.doi.org/10.1016/j.bmcl.2015.10.009>

This is a PDF file of an unedited manuscript that has been accepted for publication. As a service to our customers we are providing this early version of the manuscript. The manuscript will undergo copyediting, typesetting, and review of the resulting proof before it is published in its final form. Please note that during the production process errors may be discovered which could affect the content, and all legal disclaimers that apply to the journal pertain.



ELSEVIER

# Acyl dihydropyrazolo[1,5-*a*]pyrimidinones as metabotropic glutamate receptor 5 positive allosteric modulators

Chrysa Malosh<sup>a,b,c,d</sup>, Mark Turlington<sup>a,b,c,d</sup>, Thomas M. Bridges<sup>a,b,c</sup>, Jerri M. Rook<sup>a,b,c</sup>, Meredith J. Noetzel<sup>a,b,c</sup>, Paige N. Vinson<sup>a,b,c</sup>, Thomas Steckler<sup>e</sup>, Hilde Lavreysen<sup>e</sup>, Claire Mackie<sup>f</sup>, José M. Bartolomé-Nebreda<sup>g</sup>, Susana Conde-Ceide<sup>g</sup>, Carlos M. Martínez-Vituro<sup>g</sup>, María Piedrafita<sup>g</sup>, M. Rosa Sánchez-Casado<sup>g</sup>, Gregor J. Macdonald<sup>e</sup>, J. Scott Daniels<sup>a,b,c</sup>, Carrie K. Jones<sup>a,b,c</sup>, Colleen M. Niswender<sup>a,b,c</sup>, P. Jeffrey Conn<sup>a,b,c</sup>, Craig W. Lindsley<sup>a,b,c,d</sup> and Shaun R. Stauffer<sup>a,b,c,d\*</sup>

<sup>a</sup>Department of Pharmacology, Vanderbilt University Medical Center, Nashville, TN 37232, USA

<sup>b</sup>Vanderbilt Center for Neuroscience Drug Discovery, Vanderbilt University Medical Center, Nashville, TN 37232, USA

<sup>c</sup>Vanderbilt Specialized Chemistry Center for Probe Development (MLPCN), Nashville, TN 37232, USA

<sup>d</sup>Department of Chemistry, Vanderbilt University, Nashville, TN 37232, USA

<sup>e</sup>Neuroscience, Janssen Research and Development, Turnhoutseweg 30, B-2340, Beerse, Belgium

<sup>f</sup>Discovery Sciences ADME/Tox, Janssen Research and Development, Turnhoutseweg 30, B-2340, Beerse, Belgium

<sup>g</sup>Neuroscience Medicinal Chemistry, Janssen Research and Development, Jarama 75, 45007-Toledo, Spain

\*To whom correspondence should be addressed: shaun.stauffer@vanderbilt.edu

## ARTICLE INFO

### Article history:

Received

Revised

Accepted

Available online

### Keywords:

metabotropic glutamate receptor 5, mGlu<sub>5</sub>, positive allosteric modulator (PAM)

## ABSTRACT

We report the optimization of a series of metabotropic glutamate receptor 5 (mGlu<sub>5</sub>) positive allosteric modulators (PAMs) from an acyl dihydropyrazolo[1,5-*a*]pyrimidinone class. Investigation of exocyclic amide transpositions with this unique 5,6-bicyclic core were conducted in attempt to modulate physicochemical properties and identify a suitable backup candidate with a reduced half-life. A potent and selective PAM, 1-(2-(phenoxymethyl)-6,7-dihydropyrazolo[1,5-*a*]pyrimidin-4(5*H*)-yl)ethanone (**9a**, VU0462807), was identified with superior solubility and efficacy in the acute amphetamine-induced hyperlocomotion (AHL) rat model with a minimum effective dose of 3 mg/kg. Attempts to mitigate oxidative metabolism of the western phenoxy of **9a** through extensive modification and profiling are described.

2015 Elsevier Ltd. All rights reserved.

The pursuit of positive allosteric modulators (PAMs) of mGlu<sub>5</sub> as a promising therapeutic approach to treat cognitive deficits in schizophrenia has been stimulated by evidence from several antipsychotic and cognitive animal models.<sup>1-7</sup> Recently, we reported identification of a mGlu<sub>5</sub> PAM clinical candidate VU0409551/JNJ-46778212 (**1**)<sup>8</sup> and subsequent efforts<sup>9</sup> towards a backup candidate within the (2(phenoxymethyl)-6,7-dihydrooxazolo[5,4-*c*]pyridine-5(4*H*)-yl(aryl)methanone series focused on enhancing in vivo efficacy through improvements in PK and/or in vitro potency within the series. Prior findings from Merck-Addex<sup>10</sup> and our laboratories<sup>11</sup> unveiled a target-mediated CNS adverse-effect liability; which appeared to be driven by excessive PAM cooperativity or allosteric agonism, suggesting that PAMs with lower cooperativity and lacking allosteric agonism may be preferable for obtaining an improved therapeutic index.<sup>12,13</sup> Interestingly, electrophysiological studies with **1** indicate that signal bias may allow a path for an enhanced therapeutic window, even for PAMs with high efficacy (cooperativity/fold-shift).<sup>14</sup> Although no neurotoxicity was observed for **1** in 14 day oral dose-limiting studies in rat at 450 mg/kg/day (273-440 μM-h), IND-enabling studies at 360 mg/kg/day for 30 days (253-416 μM-h) induced Fluoro-Jade C

staining in a small number of rats, raising concerns about potential neurotoxicity sensitivity of an mGlu<sub>5</sub>PAM in man.<sup>8,14</sup>

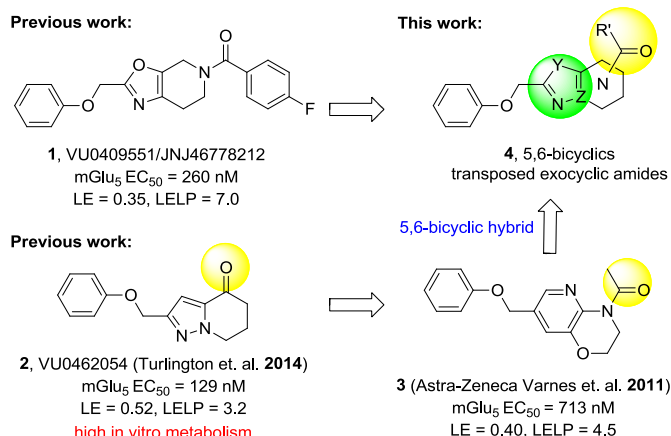
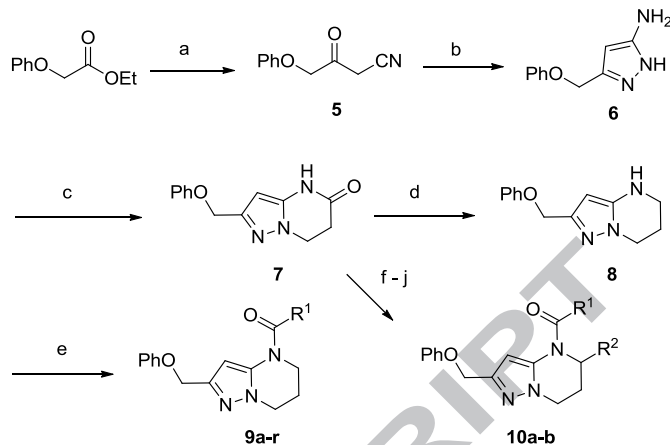


**Figure 1.** Structures, mGlu<sub>5</sub> PAM activities, and ligand efficiency metrics of clinical candidate **1** (VU0409551/JNJ-46778212), Vanderbilt ketone **2**, AZ exocyclic amide **3**, and proposed translocated amide system **4**.

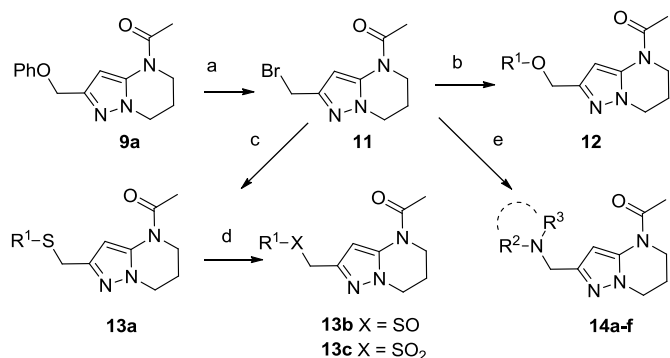
As one differentiator from the lead series we undertook the development of mGlu<sub>5</sub> PAMs with a low cooperativity profile.<sup>13</sup> However, in addition to this approach and based on our findings with **1** we wished to pursue back-up contenders specifically within other exocyclic amide subseries (**4**) that might have 1) cooperativity and signaling profiles comparable to **1**, and 2) support a shorter predicted elimination half-life in man (e.g.  $T_{1/2}$  4-6 h versus 12-24 h). Compounds with such a profile may provide a mechanism to test the hypothesis that a short-acting mGlu<sub>5</sub> PAM with a reduced in vivo residence-time and duration of action could avoid CNS toxicity while maintaining a favorable and sufficient efficacy profile. In this case, our screening paradigm consisted of traditional in vitro testing (e.g. calcium mobilization, glutamate fold-shift, mGlu selectivity assays), amphetamine-induced hyperlocomotion (AHL) challenge in rat at a single oral dose, and preclinical PK in rat and dog followed by signally pathway profiling in vitro and in more native systems for selected compounds. Previous studies in a highly efficient ketone series exemplified by PAM **2**<sup>15</sup> and the Astra-Zeneca 2,3-dihydro-1*H*-pyrido[2,3-*b*][1,4]oxazine **3**<sup>16</sup> provided the rational to initiate an amide translocation as illustrated by **4**. Compounds within template **2** were found to have high metabolic turnover relative to **1** despite excellent ligand efficiency and physicochemical properties. In the case of **2** and related congeners this was shown to be primarily connected to the oxidative liability at the benzylic ether. Therefore, backup efforts within **4** appeared to be an attractive starting point to identify shorter acting compounds with the target pharmacological profile. Similar to studies focused within ketone series **2**, the dihydropyrazolo[1,5-*a*]pyrimidine core was utilized to define a preferred translocated exocyclic amide with the target profile.

To this end we focused initially on synthesizing target **9** positioning the amide in an orientation similar to that represented by Astra-Zeneca template **3** (Scheme 1). Synthesis was envisioned to proceed in a strategy similar to that utilized in the preparation of **2**, via incorporation of the western phenoxy and building the 5,6-ring system from left to right. Initial cross-Claisen condensation using ethyl 2-phenoxyacetate and acetonitrile afforded cyano ketone **5** in 24% yield. Treatment of **5** with hydrazine in MeOH generated aminopyrazole **6** in 82% yield. Using **6**, a tandem Michael-lactam formation using methylacrylate in pyridine and water at elevated temperature proceeded in good yield to give key intermediate **7**. Lactam **7** was reduced with borane dimethyl sulfide complex to give amine **8** and subsequently coupled with acids or acyl chlorides to afford targets **9a-r**. Alternatively, treatment of lactam **7** with Boc<sub>2</sub>O, followed by Grignard addition ( $R_2MgBr$ ) and TFA treatment, furnished the desired 5-substituted 6,7-dihydropyrazolo[1,5-*a*]pyrimidine via elimination of the acyl hemiaminal. Reduction of the 6,7-dihydropyrimidine ring using Pd/C with atmospheric hydrogen followed by acylation afforded alpha 5-substituted targets **10a-b**.



**Scheme 1.** Reagents and conditions: (a) NaH, CH<sub>3</sub>CN, rt-55 °C, 4 h, 24%; (b) H<sub>2</sub>NNH<sub>2</sub>, EtOH, 85 °C, 16 h, 82%; (c) methylacrylate, pyridine, H<sub>2</sub>O, 135 °C, 48 h, 75%; (d) BH<sub>3</sub>-SMe<sub>2</sub>, THF, 0 – 60 °C, 16 h, 95%; (e) R<sup>1</sup>COCl, DCM, Et<sub>3</sub>N or R<sup>1</sup>CO<sub>2</sub>H, Ghosez reagent, DMF, DIPEA, 0 °C – rt, 25-70%; (f) Boc<sub>2</sub>O, THF, 76%; (g) R<sub>2</sub>MgBr, THF, 0 °C, 33-61%; (h) TFA, DCM, 0 °C, 64-71%; (i) Pd/C, H<sub>2</sub>, EtOAc, 82%; (j) R<sup>1</sup>COCl, DCM, Et<sub>3</sub>N, 0 °C – rt, 22-58%.

To access western phenoxy and various linker analogs in parallel, compound **9a** was deprotected using BBr<sub>3</sub> at low temperature to afford bromide **11** in moderate yield (55%, Scheme 2). Displacement of bromide **11** with alcohols, thiols, and amines proceeded smoothly to afford analogs (**12-14**). Sulfide **13a** could be subsequently oxidized using one or two equivalents of MCPBA to afford sulfone **13b** and sulfoxide **13c**, respectively.



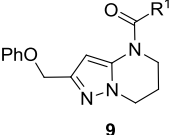
**Scheme 2.** Reagents and conditions: (a) BBr<sub>3</sub>, DCM, 0 °C, 3 h, 55% (b) R<sup>1</sup>OH, DMF, K<sub>2</sub>CO<sub>3</sub>, 140 °C μwave, 20 min., 33-84%; (c) R<sup>1</sup>SH, CH<sub>3</sub>CN, 120 °C μwave, 20 min., 81%; (d) MCPBA 1 or 2 equiv, DCM, -20 °C – rt, 2 h, 24-68, (e) R<sub>2</sub>R<sub>3</sub>NH, DMF, K<sub>2</sub>CO<sub>3</sub>, rt, 4-16h, 45-76%.

Gratifyingly, the translocated exocyclic amide concept **4** proved successful within the dihydropyrazolo pyrimidine core as acetylated analog **9a** (Table 1), a close comparator to AZ-ether **3**, was a PAM with an EC<sub>50</sub> of 360 nM and good efficacy (65% Glu Max). Importantly, no allosteric agonism was detected in cell lines over expressing mGlu<sub>5</sub> or in rat astrocytes, which represents a native tissue setting in which mGlu<sub>5</sub> is endogenously expressed (vida infra Fig. 4). In addition, based on potency, MW, and physicochemical properties (cLogP = 2.1), **9a** displayed excellent ligand efficiency metrics (LE = 0.44, LELP = 4.7) comparable to **2** and **3**, thus making it an attractive starting point for further optimization. With exception of ethyl congener **9b** (EC<sub>50</sub> = 332 nM), higher alkyl homologs of **9a** proved deleterious; with diminished potency tracking with increasing steric bulk near the amide (**9c** versus **9d**). Saturated carbocycles revealed a similar trend (**9e-9g**); cyclopropyl was preferred (**9e**, EC<sub>50</sub> = 559 nM) with potency comparable to methyl (**9a**) and ethyl (**9b**) congeners. Interestingly, phenyl acetate analog **9h** produced a PAM with potency similar to lead **9a** (EC<sub>50</sub> = 378 nM) at the

obvious cost of ligand efficiency. With respect to aryl moieties, SAR was flat (**9i-9m**) with no general improvements in activity. A low efficacy thiazoly amide **9r** ( $EC_{50} = 257$  nM, Glu Max = 24%) was identified; however, heterocyclic amides more typically displayed weak (isoxazolyl **9q**, pyridyl **9n**, **9o**) or inactive (furan **9p**) profiles. In contrast to SAR within the ketone series **2**, introduction of alpha substituents within the 6,7-dihydropyrazolo[1,5-a]pyrimidine (**Fig. 2**) including 5-methyl (**10a**) and 5-phenyl (**10b**) were flat or lost activity versus **9a**, possibly indicating disruption of a preferred amide conformation.

Utilizing **11** and the method described in Scheme 2 a thorough examination of western phenoxy SAR was undertaken and is shown in Table 2. Fluorine walk within series **12** revealed a strict preference for 3-fluoro congener (**12b**,  $EC_{50} = 266$  nM) as 2-fluoro (**12a**) and 4-fluoro (**12c**) derivatives were weak or inactive. In addition, di-substitution as either difluoro (**12d**) or 3-cyano-5-fluoro (**12e**) afforded weak PAMs and pyridyl derivatives **12f-g** were unproductive. Intermediate **11** was also utilized to revisit broader linker SAR and, in the case of thioether **13a**, weak PAM activity was observed, while the corresponding sulfone (**13b**) and sulfoxide (**13c**) were inactive.

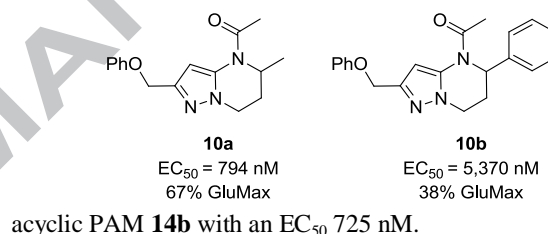
**Table 1.** Structures and activities of analogs **9**.

				
Entry	R <sup>1</sup>	pEC <sub>50</sub> <sup>a</sup>	EC <sub>50</sub> (nM) <sup>a</sup>	Glu Max % <sup>a</sup>
<b>9a</b>		6.44±0.04	360	65±3
<b>9b</b>		6.48±0.03	332	48±5
<b>9c</b>		5.77±0.11	1,710	59±4
<b>9d</b>		6.05±0.09	882	64±2
<b>9e</b>		6.28±0.05	559	61±6
<b>9f</b>		5.91±0.12	1,220	41±8
<b>9g</b>		5.76±0.11	1,750	41±11
<b>9h</b>		6.43±0.03	378	72±4
<b>9i</b>		6.21±0.06	610	63±5
<b>9j</b>		5.95±0.08	1,130	62±5
<b>9k</b>		6.23±0.07	591	61±6
<b>9l</b>		6.22±0.05	596	63±8
<b>9m</b>		6.41±0.04	390	68±3
<b>9n</b>		<5.00	>10,000	44±11

<b>9o</b>		<5.00	>10,000	51±9
<b>9p</b>		<4.5	Inactive	<15
<b>9q</b>		5.56±0.11	2780	22±7
<b>9r</b>		6.59±0.02	257	24±7

<sup>a</sup>Calcium mobilization assay using HEK293 cells expressing human mGlu<sub>3</sub>; values are the mean±SEM of three or more independent determinations performed in triplicate.

A brief survey of amines proved more interesting as ether linkage replacements. Aniline **14a** demonstrated weak PAM activity; however, the *N*-methyl aniline **14b** displayed robust efficacy (Glu Max = 74%) and an  $EC_{50}$  of 700 nM. Attempts to replace the aniline moiety with a [1.1.1] propellane to afford **14c** proved unsuccessful. A series of constrained anilines were then explored to expand **14b**. Indoline **14d** was inactive; however, tetrahydroquinoline (**14e**) displayed weak PAM activity. Based on the weak activity of **14e**, benzoxazine **14f** was prepared to further explore alternative six-member constraints. Gratifyingly, **14f** demonstrated comparable potency and efficacy versus the



acyclic PAM **14b** with an  $EC_{50}$  725 nM.

**Figure 2.** Structures and activities of 5-substituted analogs **10**.

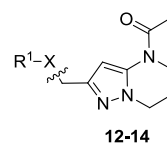


**Table 2.** Structures and activities of linker analogs **12-14**.

Entry	R <sup>1</sup> X-	pEC <sub>50</sub> <sup>a</sup>	EC <sub>50</sub> (nM) <sup>a</sup>	Glu Max % <sup>a</sup>
<b>12a</b>		5.63±0.13	2,370	60±6
<b>12b</b>		6.62±0.03	266	58±8
<b>12c</b>		<5.00	>10,000	56±4
<b>12d</b>		5.90±0.06	1,270	63±3
<b>12e</b>		<5.00	>10,000	39±9
<b>12f</b>		<4.5	Inactive	<15
<b>12g</b>		<4.5	Inactive	<15
<b>13a</b>		5.41±0.16	3,900	39±8



<b>13b</b>		<4.5	Inactive	<15
<b>13c</b>		<4.5	Inactive	<15
<b>14a</b>		<5.00	>10,000	20±6
<b>14b</b>		6.15±0.06	700	74±3
<b>14c</b>		<4.5	Inactive	<15
<b>14d</b>		<4.5	Inactive	<15
<b>14e</b>		<5.00	>10,000	48±12
<b>14f</b>		6.14±0.07	725	67±4

<sup>a</sup>Calcium mobilization assay using HEK293 cells expressing human mGlu<sub>5</sub>; values are the mean±SEM of three or more independent determinations performed in triplicate.

We next evaluated the in vitro DMPK profiles of selected analogs including **9a**, **12b**, **14b**, and **14f** (Table 3). In hepatic microsomal intrinsic clearance assays, both phenoxy PAMs **9a** and **12b** displayed moderate to high in vitro metabolism with predicted hepatic clearance ( $CL_{HEP}$ ) > 35 mL min<sup>-1</sup> kg<sup>-1</sup> in rat and > 12 mL min<sup>-1</sup> kg<sup>-1</sup> in human. Both amino congeners **14b** and **14f** displayed higher turnover in rat, with similar turnover in human near 50% maximum liver blood flow. Plasma protein binding experiments revealed high fraction unbound in both rat and human plasma for all four compounds (24-43% unbound in rat plasma, 17-46% unbound in human plasma). A rat PK study (0.2 mg/kg, intravenous cassette paradigm, male Sprague-Dawley,  $n = 2$ ) using **9a** and **12a** confirmed high clearance in vivo with super hepatic clearance (rat  $CL_p$  > 70 mL min<sup>-1</sup> kg<sup>-1</sup>). Follow up rat plasma stability studies indicated both **9a** and **12a** were stable (4 h incubation; 37 °C). Further stability studies in simulated gastric fluid for 1 h (SGF solubility 315 µg/mL, 37 °C) or in vehicle formulations (20% β-CD pH 6, 4 mg/mL) for up to five days also indicated the external amide remained intact with < 5% decomposition. In parallel, both **9a** and **12a** were evaluated in vivo in an amphetamine-induced hyperlocomotion (AHL) challenge model using an oral screening dose of 10 mg/kg.<sup>17</sup> Interestingly as shown in Table 3, **9a** demonstrated a robust 20% reversal of AHL while **12a** was without effect relative to vehicle control (<10% reversal). Terminal mean brain and plasma levels ( $n = 6$  animals,  $T_{90}$ ) were assessed from these studies to inform interpretation of the screening results. PAM **9a** exhibited a terminal brain concentration of 2.25 µM and plasma concentration of 2.15 µM, corresponding to an estimated unbound brain concentration of 1.16 µM (based on a rat  $f_{u, brain} = 0.51$  from brain homogenate binding assay), while the corresponding 3-fluoro derivative **12a** was not detected in brain samples. Thus, based on the performance of **9a** in our pharmacodynamic screen and its apparent enhanced CNS penetration (calculated  $K_{p,uu}$  of 1.4),<sup>18</sup> we opted to further profile **9a** in additional pharmacological endpoints, discrete PK (rat and dog), and in full dose-response studies in rat AHL to determine its minimal effective dose (MED). The dose response profile for **9a** in AHL with unbound terminal brain concentrations is shown in Figure 3 along with an extensive profile overview in Figure 4.

**Table 3.** In vitro DMPK, rat IV pharmacokinetics, and rat amphetamine-induced locomotion % reversal from 10 mg/kg PO: **9a**, **12b**, **14c**, and **14f**.<sup>a</sup>

Entry	$CL_{int}$ (h, r) <sup>b</sup>	$CL_{hep}$ (h, r) <sup>b</sup>	PPB $f_u$ (h, r)	Rat $CL_p$ <sup>c</sup>	AHL $T_{90}$ % reversal <sup>d</sup>
<b>9a</b>	21, 74	12, 36	0.26, 0.37	118	20
<b>12a</b>	23, 62	11, 42	0.17, 0.24	103	<10
<b>14b</b>	18, 269	9, 56	0.46, 0.35	nt	nt
<b>14f</b>	25, 225	12, 53	0.35, 0.43	nt	nt

<sup>a</sup>human (h), rat (r), dog (d); <sup>b</sup>mL/min/kg, see Ref. 13 and 17 for methods; <sup>c</sup>mL/min/kg, rat IV dose 0.2 mg/kg; <sup>d</sup>amphetamine-induced locomotion % reversal see Ref 12, vehicle 20% HP-β-CD; nt= not tested.

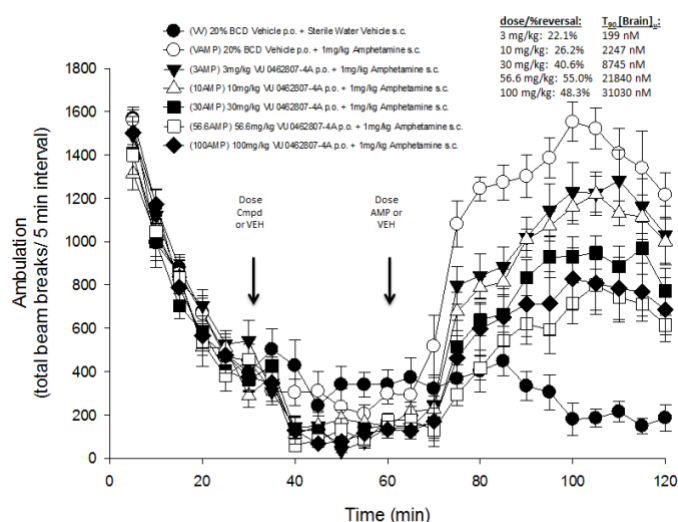


**Figure 3.** Dose-dependent reversal effect and calculated terminal unbound brain levels of **9a** in AHL in male, SD rats after oral administration ( $n = 8$  animals/group).

As seen from Figure 3, **9a** displayed a maximum reversal of 55% at a dose of 56.6 mg/kg and a 22% reversal at an MED of 3 mg/kg. At the 3 mg/kg dose, this corresponds to a terminal estimated unbound brain concentration of 199 nM, a three-fold multiple of the rat mGlu<sub>5</sub> potency of 60 nM (Figure 4). To the best of our knowledge, only **9a** and one other dihydroimidazopyrimidinone mGlu<sub>5</sub> PAM from a lactam class<sup>19</sup> have demonstrated an MED of 3 mg/kg (PO) in the AHL antipsychotic efficacy model; however, in the latter case, dihydroimidazopyrimidinone mGlu<sub>5</sub> PAMs<sup>19</sup> showed clear CNS-mediated side effects in dog and in rat modified Irwin test batteries thought to be attributed to high cooperativity and/or mixed mGlu<sub>5</sub>/mGlu<sub>3</sub> activity. Evaluation of **9a** in a rat modified Irwin study using a 30 mg/kg PO dose demonstrated no observable alterations in behavior across 30 distinct autonomic and somatomotor endpoints. In this study, **9a** reached an impressive brain concentration of 71 µM 1.0 h post-dose (est.  $C_{b,u} = 36$  µM). At a dose of 56.6 mg/kg, 113 µM of **9a** was measured in the brain (est.  $C_{b,u} = 67$  µM) and a modified Racine score of 1 noted over a 6.0 h observational period, with animals generally demonstrating decreased motor activity and coordination. Based on the concentrations achieved in the modified Irwin studies and in the AHL dose-response study at the MED, **9a** appeared to provide a large safety window, in this case 100-fold or greater on the basis of these acute testing paradigms. Thus, PAM **9a** represented a considerable improvement relative

to candidate **1** (MED of 10 mg/kg)<sup>8</sup> or related back-up candidates (MEDs of 30 mg/kg)<sup>9</sup> on the basis of AHL and behavioral CNS toxicity.

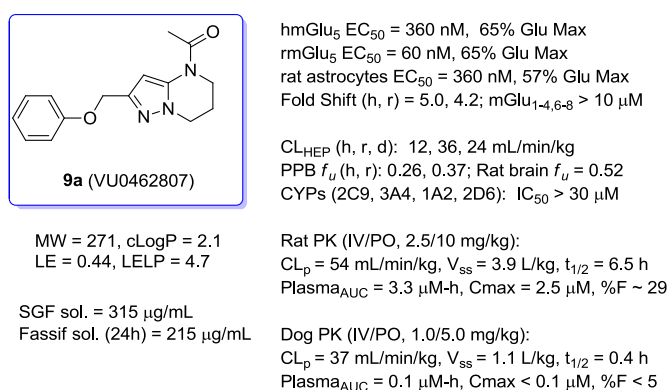


**Figure 4.** In vitro and in vivo profile summary of **9a**.

Further pharmacological profiling of **9a** in glutamate concentration response curve (CRC) fold-shift experiments with human or rat mGlu<sub>5</sub> receptor expressing cell lines revealed modest maximal leftward fold-shifts (FS) of 5.0 and 4.2 respectively, using 10 µM of PAM (**Fig. 4**). PAM **9a** was also highly selective versus other mGlu family members (mGlu<sub>1-4,6-8</sub> FS < 1.2) and no noted activity was observed in a broad panel ancillary screen against 68 distinct GPCRs, ion channels and transporters (Eurofins Inc.). In addition, **9a** had an excellent profile against the major CYP<sub>450</sub> enzymes (>30 µM IC<sub>50</sub>s). Evaluation of **9a** in discrete rat and dog pharmacokinetic studies confirmed the inherent moderate to high clearance of **9a** in both species (**Fig. 4**); however, in rat the elimination *T*<sub>1/2</sub> was 6.5 h, a profile consistent with this particular backup effort. After oral administration (10 mg/kg, 20% β-CD, 1 mg/mL) to male Sprague-Dawley rats, **9a** reached an average maximal concentration (*C*<sub>max</sub>) of 2.5 µM with a corresponding time to reach *C*<sub>max</sub> (*T*<sub>max</sub>) of 1.0 h and an AUC<sub>0-8h</sub> of 3.31 µM-h, thus affording an absolute %F of 29. Unfortunately, in dog both IV and oral PK proved disappointing, with **9a** exhibiting both poor exposure and low bioavailability and a short elimination *T*<sub>1/2</sub> of less than 30 minutes.

Despite promising CNS penetration and acute efficacy in vivo in rat AHL, ongoing backup efforts progressing PAM **9a** or related members of the series were considered challenging given the poor dog PK and steep SAR. Similar to prior studies in lead candidate series **1** and within the ketone series **2**, in vitro metabolic soft-spot analysis revealed oxidative metabolism of the electron rich western phenoxy moiety, in addition to the C(4) pyrazole carbon, as major contributors to the observed metabolic instability.

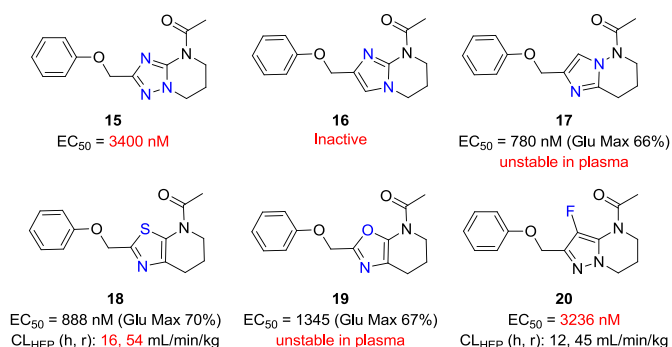


**Figure 5.** Isosteric replacements **15-19** and fluoro derivative **20**.

In light of the limited success in addressing the metabolic soft-spot through modification of the western phenoxy ring both herein (e.g. Table 2) and in previous subseries,<sup>9,15</sup> the medicinal chemistry campaign focused on attempting to mitigate metabolic turnover through modifications of the pyrazole core itself and through modification of the pyrazolo C(4) carbon. Efforts in this vein are briefly summarized in Figure 5. Despite considerable attempts to modify the nature of the heterocyclic core structure (**Fig. 5, 15-19**) or substitute the C(4) position of **9a** with fluorine (**20**), these efforts generally resulted in compounds that suffered from diminished PAM activity or from metabolic and/or plasma instability.

In summary, we have discovered a set of potent mGlu<sub>5</sub> PAMs with high ligand efficiency and excellent CNS penetration inspired by the exocyclic amide **3** and conceptually by the hybrid 5,6-bicyclic template **4**. In an effort to identify PAMs with reduced half-lives and pharmacological target profiles most similar to candidate **1**, PAM **9a** (VU0462807) was identified as a selective and moderate fold-shift mGlu<sub>5</sub> PAM having an exquisite efficacy profile in the acute AHL rat model. Despite our success in identifying a centrally penetrant compound with both improved in vivo potency and a reduced half-life, the overall metabolic instability and correspondingly poor oral F in higher species was deemed unacceptable for development and thus backup efforts in this area were suspended. Ongoing studies utilizing **9a** for other indications and additional chronic studies to better understand PK/PD and duration of action are ongoing and will be communicated in due course.

## Supporting information

Synthesis and experimental details for **9a** and **20**, along with routes and conditions used to prepare heterocycles **15-19** are available as supporting information.

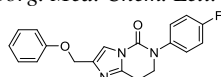
## Acknowledgments

Vanderbilt Center for Neuroscience Drug Discovery (VCNDD) research was supported by grants from Janssen, The Pharmaceutical Companies of Johnson & Johnson and in part by the NIH (NS031373, MH062646).

## References and Notes

- Awad, H.; Hubert, G. W.; Smith, Y.; Levey, A. I.; Conn, P. J. *J. Neurosci.* **2000**, *20*, 7871.
- Chavez-Noriega, L. E.; Schaffhauser, H.; Campbell, U. C. *Curr Drug Targets CNS Neurol. Disord.* **2002**, *1*, 261.
- Perroy, J.; Raynaud, F.; Homburger, V.; Rousset, M. C.; Telley, L.; Bockaert, J.; Fagni, L. *J. Biol. Chem.* **2008**, *283*, 6799.
- Conn, P. J.; Lindsley, C. W.; Jones, C. K. *Trends Pharmacol. Sci.* **2009**, *30*, 25.
- Rosenbrock, H.; Kramer, G.; Hobson, S.; Koros, E.; Grundl, M.; Grauert, M.; Reymann, K. G.; Schroder, U. H. *Eur J Pharmacol.* **2010**, *639*, 40.
- Stauffer, S. R. *ACS Chem. Neurosci.* **2011**, *2*, 450.
- Lindsley, C. W.; Stauffer, S. R. *Pharmaceutical Patent Analyst* **2013**, *2*, 93.
- Conde-Ceide, S.; Martinez-Vituro, C. M.; Alcazar, J.; Garcia-Barrantes, P. M.; Lavreysen, H.; Mackie, C.; Vinson, P. N.; Rook, J. M.; Bridges, T. M.; Daniels, J. S.; Megens, A.; Langlois, X.; Drinkenburg, W. H.; Ahnaou, A.; Niswender, C. M.; Jones, C. K.; Macdonald, G. J.; Steckler, T.; Conn, P. J.; Stauffer, S. R.; Bartolome-Nebreda, J. M.; Lindsley, C. W. *ACS Med. Chem. Letters* **2015**, *6*, 716.

9. Zhou, Y.; Malosh, C.; Conde-Ceide, S.; Martinez-Vituro, C. M.; Alcazar, J.; Lavreysen, H.; Mackie, C.; Bridges, T. M.; Daniels, J. S.; Niswender, C. M.; Jones, C. K.; Macdonald, G. J.; Steckler, T.; Conn, P. J.; Stauffer, S. R.; Bartolome-Nebreda, J. M.; Lindsley, C. W. *Bioorg. Med. Chem. Lett.* **2015**, *17*, 3515-3519.
10. Parmentier-Batteur, S.; Hutson, P. H.; Menzel, K.; Uslander, J. M.; Mattson, B. A.; O'Brien, J. A.; Magliaro, B. C.; Forest, T.; Stump, C. A.; Tynebor, R. M.; Anthony, N. J.; Tucker, T. J.; Zhang, X. F.; Gomez, R.; Huszar, S. L.; Lambeng, N.; Faure, H.; Le Poul, E.; Poli, S.; Rosahl, T. W.; Rocher, J. P.; Hargreaves, R.; Williams, T. M. *Neuropharmacology* **2014**, *82*, 161-173.
11. Rook, J. M.; Noetzel, M. J.; Pouliot, W. A.; Bridges, T. M.; Vinson, P. N.; Cho, H. P.; Zhou, Y.; Gogliotti, R. D.; Manka, J. T.; Gregory, K. J.; Stauffer, S. R.; Dudek, F. E.; Xiang, Z.; Niswender, C. M.; Daniels, J. S.; Jones, C. K.; Lindsley, C. W.; Conn, P. J. *Biol. Psychiatry* **2013**, *73*, 501.
12. Turlington, M.; Noetzel, M. J.; Chun, A.; Zhou, Y.; Gogliotti, R. D.; Nguyen, E. D.; Gregory, K. J.; Vinson, P. N.; Rook, J. M.; Gogi, K. K.; Xiang, Z.; Bridges, T. M.; Daniels, J. S.; Jones, C.; Niswender, C. M.; Meiler, J.; Conn, P. J.; Lindsley, C. W.; Stauffer, S. R. *J. Med. Chem.* **2013**, *56*, 7976.
13. Turlington, M.; Malosh, C.; Jacobs, J.; Manka, J. T.; Noetzel, M. J.; Vinson, P. N.; Jadhav, S.; Herman, E. J.; Lavreysen, H.; Mackie, C.; Bartolome-Nebreda, J. M.; Conde-Ceide, S.; Martin-Martin, M. L.; Tong, H. M.; Lopez, S.; Macdonald, G. J.; Steckler, T.; Daniels, J. S.; Weaver, C.; Niswender, C. M.; Jones, C.; Conn, P. J.; Lindsley, C. W.; Stauffer, S. R. *J. Med. Chem.* **2014**, *57*, 5620.
14. Rook, J. M.; Xiang, Z.; Lv, X.; Ghoshal, A.; Dickerson, J. W.; Bridges, T. M.; Johnson, K. A.; Foster, D. J.; Gregory, K. J.; Vinson, P. N.; Thompson, A. D.; Byun, N.; Collier, R. L.; Bubser, M.; Nedelcovych, M. T.; Gould, R. W.; Stauffer, S. R.; Daniels, J. S.; Niswender, C. M.; Lavreysen, H.; Mackie, C.; Conde-Ceide, S.; Alcazar, J.; Bartolome-Nebreda, J. M.; Macdonald, G. J.; Talpos, J. C.; Steckler, T.; Jones, C. K.; Lindsley, C. W.; Conn, P. J. *Neuron* **2015**, *86*, 1029.
15. Turlington, M.; Noetzel, M. J.; Bridges, T. M.; Vinson, P. N.; Steckler, T.; Lavreysen, H.; Mackie, C.; Bartolome-Nebreda, J. M.; Conde-Ceide, S.; Tong, H. M.; Macdonald, G. J.; Daniels, J. S.; Jones, C. K.; Niswender, C. M.; Conn, P. J.; Lindsley, C. W.; Stauffer, S. R. *Bioorg. Med. Chem. Lett.* **2014**, *24*, 3641.
16. Varnes, J. G.; Marcus, A. P.; Mauger, R. C.; Throner, S. R.; Hoesch, V.; King, M. M.; Wang, X.; Sygowski, L. A.; Spear, N.; Gadiant, R.; Brown, D. G.; Campbell, J. B. *Bioorg. Med. Chem. Lett.* **2011**, *21*, 1402.
17. Kinney, G. G.; O'Brien, J. A.; Lemaire, W.; Burno, M.; Bickel, D. J.; Clements, M. K.; Chen, T. B.; Wisnoski, D. D.; Lindsley, C. W.; Tiller, P. R.; Smith, S.; Jacobson, M. A.; Sur, C.; Duggan, M. E.; Pettibone, D. J.; Conn, P. J.; Williams, D. L., Jr. *J. Pharmacol. Exp. Ther.* **2005**, *313*, 199.
18. Di, L.; Rong, H.; Feng, B. *J. Med. Chem.* **2013**, *56*, 2.
19. Martin-Martin, M. L.; Bartolome-Nebreda, J. M.; Conde-Ceide, S.; Alonso de Diego, S. A.; Lopez, S.; Martinez-Vituro, C. M.; Tong, H. M.; Lavreysen, H.; Macdonald, G. J.; Steckler, T.; Mackie, C.; Bridges, T. M.; Daniels, J. S.; Niswender, C. M.; Noetzel, M. J.; Jones, C. K.; Conn, P. J.; Lindsley, C. W.; Stauffer, S. R. *Bioorg. Med. Chem. Lett.* **2015**, *25*, 1310.



**4a**  
mGlu<sub>5</sub> EC<sub>50</sub> = 86 nM  
FS = 12.5 (10  $\mu$ M)

20. Bridges, T. M.; Rook, J. M.; Noetzel, M. J.; Morrison, R. D.; Zhou, Y.; Gogliotti, R. D.; Vinson, P. N.; Xiang, Z.; Jones, C. K.; Niswender, C. M.; Lindsley, C. W.; Stauffer, S. R.; Conn, P. J.; Daniels, J. S. *Drug Metab. Dispos.* **2013**, *41*, 1703.

## Graphical Abstract

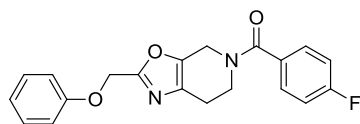
To create your abstract, type over the instructions in the template box below.

Fonts or abstract dimensions should not be changed or altered.

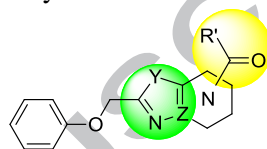
### Acyl dihydropyrazolo[1,5-a]pyrimidinones as metabotropic glutamate receptor 5 positive allosteric modulators

Leave this area blank for abstract info.

Chrysa Malosh, Mark Turlington, Thomas M. Bridges, Jerri M. Rook, Meredith J. Noetzel, Paige N. Vinson, Thomas Steckler, Hilde Lavreysen, Claire Mackie, José M. Bartolomé-Nebreda, Susana Conde-Ceide, Carlos M. Martínez-Vituro, María Piedrafita, M. Rosa Sánchez-Casado, Gregor J. Macdonald, J. Scott Daniels, Carrie K. Jones, Colleen M. Niswender, P. Jeffrey Conn, Craig W. Lindsley and Shaun R. Stauffer



VU0409551/JNJ46778212  
mGlu<sub>5</sub> PAM clinical candidate



transposed exocyclic amides

\*improved in vivo efficacy

\*reduced elimination  $T_{1/2}$